JTTEES 7:392-402

Particle Temperature and Flux Measurement Utilizing a Nonthermal Signal Correction Process

K. Hollis and R. Neiser

(Submitted 2 January 1998; in revised form 17 March 1998)

In-flight measurement of the surface temperature of plasma-sprayed particles is important for the correlation of particle characteristics to coating structure and properties. However, the use of optical pyrometry for particle surface temperature measurement has inherent uncertainties due to nonthermal emission signals in the plasma/particle plume. This nonthermal signal is especially pronounced near the torch exit and in regions of the plume where there are few particles. This work shows that both plasma and particle vapor signals in the form of line emission and continuum emission can be compensated for when calculating particle temperatures from the emission of the plasma/particle plume. The nonthermal signals have been estimated and removed from the raw spectral data, producing a more accurate calculated particle temperature. Using spectral shape fitting to determine the particle temperatures allows the radiant intensity to be used for particle flux estimation, thus providing more information on the state of the particle plume. Additionally, the spectral emittance of molybdenum particles sprayed in air was found to more closely resemble the emittance of pure molybdenum than the emittance of MoO_3.

Keywords	diagnostic, flux, multi-color pyrometry, nonthermal correction, particle

1. Introduction

The in-flight temperature of plasma-sprayed particles is an important parameter to be measured to better understand the plasma-spraying process. Particle temperature has been shown to be an important parameter in predicting particle flattening (Ref 1), and is thought to play a major role in coating formation (Ref 2). Therefore, an accurate measurement of particle temperature is needed in order to determine a reliable correlation between in-flight particle temperatures and coating structure and properties.

The measurement of particle temperature by optical pyrometry has been accomplished by researchers using various methods. For example, see Ref 3 to 5. Inherent in the optical pyrometric method are sources of error in the temperature calculation. The error arises from the collection and analysis of the optical emission signal. Along with the particle thermal emission signal, other "nonthermal" emission signals are collected. Failure to identify and remove the nonthermal signals leads to errors in calculated particle surface temperatures. The effect of nonthermal signals is especially large near the plasma torch exit or in regions where there are few or relatively cool particles. Therefore, the need exists to identify the nonthermal signals and to devise a way of subtracting them from the collected optical signals used for particle pyrometry, in order to improve particle surface temperature measurements.

An accompanying paper (Ref 6) presents a method for identifying and quantifying the nonthermal signals present in the spectra collected from an argon/helium plasma plume laden with molybdenum particles. That work, along with earlier results from this investigation (Ref 7), has provided the understanding needed for the work presented in this paper. The work presented here describes a method for estimating the nonthermal signals present in collected emission spectra from the plasma/particle plume. Once identified, the nonthermal signals are subtracted from the raw data to give a more realistic representation of the thermal emission of the particles, resulting in more accurate particle surface temperature calculations. Additionally, because the spectral shape of the thermal emission signal is used to determine the particle temperatures, the radiant intensity is used for particle flux estimation and thus provides more information on the state of the particle plume.

K. Hollis, Los Alamos National Laboratory, MST-6 Metallurgy, MS G-770, PO Box 1663, Los Alamos, NM 87545, USA; **R. Neiser,** Sandia National Laboratory, Albuquerque, NM. Contact e-mail: khollis@lanl.gov.

2. Background

An optical pyrometer uses a measurement of the thermal radiation emitted from an object to determine the temperature of the object's surface. The relation between the spectral thermal emission and the temperature of the particle is determined by the specific thermal radiative properties of the material and the laws of thermal radiation heat transfer. The spectral or wavelength distribution of the emitted thermal flux is given by the Planck equation

$$M_\lambda = \varepsilon(T,\lambda)c_1\lambda^{-5}[\exp(c_2/\lambda T) - 1]^{-1} \quad \text{(Eq 1)}$$

where M_λ is the spectral thermal emission intensity, c_1 is the first radiation constant, c_2 is the second radiation constant, λ is the wavelength of the radiation, T is the absolute surface temperature, and $\varepsilon(T,\lambda)$ is the proportionality factor for non-blackbodies, known as the emittance, which is a function of wavelength and temperature. Collecting the emitted thermal radiation at a known wavelength from a particle with a known emittance al-

lows for the calculation of the particle surface temperature from the Planck equation.

When collecting the thermal emission signals from particles in a plasma plume, several nonthermal signals are also collected, including:

- The line and continuum emission from the plasma surrounding the particles in the detector sampling volume
- The line and continuum emission from the intensely bright arc and plasma in the throat of the gun which is reflected into the detector by the particles that act as radiation scatterers
- The line and continuum emission from the vaporized particle material that is spread throughout the plume

Several authors have pointed out that the primary limitation in measuring particle emission is the presence of the bright plasma near the exit of the plasma torch (Ref 3-5). Sakuta and Boulos (Ref 8) have calculated the relative intensities of plasma and particle emission in the detector field of view in an effort to determine where the plasma signal drowns out the particle thermal emission. Gougeon and Moreau (Ref 9) have calculated the amount of particle-reflected plasma radiation that is collected with the thermal emission. Their calculations showed that the particle-reflected radiation can represent a significant source of temperature calculation error. The smaller, cooler, and closer to the torch exit plane the particle is, the more significant the error. However, from a simulated particle signal reflection measurement, Prucha and Skarda (Ref 10) concluded that the plasma light scattered by the particles does not need to be considered for in-flight particle pyrometry. Clearly, more accurate measurement of the nonthermal signals present will help to better understand the limitations of in-flight particle pyrometry. Furthermore, if the nonthermal signals can be subtracted from the raw collected signals, more accurate temperature measurements can be made.

In order to gain an understanding of the influence on particle temperature measurements of the various sources of radiation present in the plasma/particle plume, optical sampling must take place over a broad spectral range, with sufficient precision within the range to identify characteristic line emission. For this investigation, radiation in the range of 340 to 640 nm was sampled with a spectral resolution of 0.36 nm. Longer wavelengths were avoided due to the numerous argon lines present. Quickly collecting data over such a range necessitates the use of multiple detectors. Here, an intensified 1024 element linear diode array detector was used for data collection. However, the low sensitivity of the diodes precluded the resolution of single-particle emission spectra. So, the emission from many particles passing through the sampling volume was recorded for each location in the plume. Thus, the method of optical sampling used for this investigation is best described as multicolor, multiparticle. The method is similar to that used by Kuroda et al. (Ref 4).

Radiation emission observed from a particle-laden plasma-spray plume emanates from matter in the solid, liquid, vapor, and plasma states. The emission from the solid and liquid phases is due to the thermal emission from particles and is treated in this paper. Analysis of the radiation emitted from the vapor and plasma states, along with a description of the sources of the observed radiation, are given in an accompanying paper (Ref 6).

3. Data Collection

The experimental conditions are the same as listed in the accompanying paper (Ref 6) and will be described only briefly here. The plasma torch used for this experiment was the commercially available Miller Thermal, Inc. SG-100 (Appleton, WI). The torch parameters used are listed in Table 1. The powder used was Miller Thermal, Inc. AI-1013 molybdenum which was cut to a 63 to 75 μm diameter size distribution. The powder feed rate was a relatively low 10 g/min. Spraying was carried out in the local atmospheric pressure of 90 kPa (Albuquerque, NM). The optical sampling equipment setup is shown in Fig. 1. The light shield, light trap, and tubes covering the optic path were used to reduce detection of room-reflected light. The optical detection system chosen for this experiment was a 1/3 m focal length spectrograph (Thermo Jarrell Ash 82-498; Franklin, MA), with an intensified 1024 element linear diode array (Tracor Northern; Middleton, WI). The signals from the diodes were fed into a detector controller and then into a personal computer for storage. Also shown in Fig. 1 are the optical components used in collecting the radiation to be analyzed. The collection lens was a 209 mm, f/4.5 photographic lens. When recording spectra, five exposures were taken sequentially and averaged. This averaged data was used for all subsequent analysis. The integration time of the sampling was between 0.01 and 1.1 s/exposure, so many particles were detected in a single spectrum.

The optical system was calibrated for both wavelength and spectral sensitivity. The diode signals were calibrated for wavelength using calibration lamps which provide line emission at known wavelengths. The spectral sensitivity of the optical

Table 1 SG-100 torch parameters

Parameter	Value
Torch current	795 A
Torch voltage	36.6 V
Argon arc gas flow rate	40.1 slm(a)
Helium arc gas flow rate	24.1 slm(a)
Argon powder gas flow rate	3.8 slm(a)
Anode/cathode/gas injector	720/730/112(b)

(a) Standard liters per minute. (b) Miller Thermal, Inc., part numbers

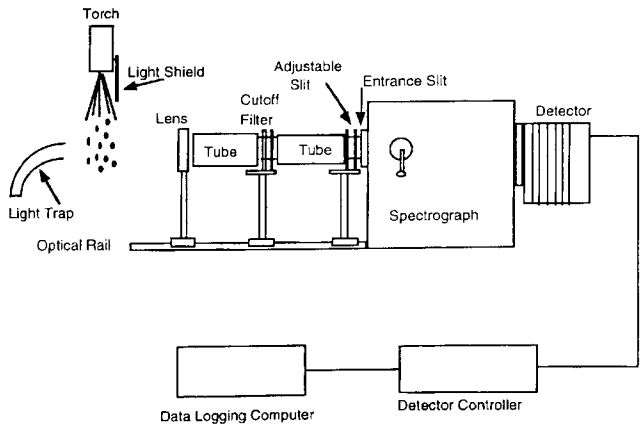

Fig. 1 Experimental setup for optical sampling

detection system was determined using a tungsten strip lamp traceable to a National Institute of Standards and Technology calibration. With the known lamp output, the instrument response function (IRF) for the optical components and the detection system was determined.

The spatial data sampling coordinates are shown in Fig. 2. Data were taken between x = 50 and 200 mm. Spectra were recorded at vertical y-coordinate increments of 1.09 mm. Two types of spectra were recorded. The first type was recorded with particles in the plasma and is referred to as a "with-particle" spectrum. The second type of spectrum was recorded at the same location as the with-particle spectrum, but no particles were injected into the plasma during data collection. This type of spectrum is called a "without-particle" spectrum.

4. Analysis and Discussion

4.1 Separation of Nonthermal Signals

The with-particle spectra show that the plasma and vapor signals present are easily observed by identifying the plasma gas or particle vapor characteristic emission lines. In addition to the lines which are easily visible, there is some combination of plasma and vapor continuum emission in the collected spectra. The continua represent another nonthermal radiation source which will cause errors in the particle temperature calculation if not removed from the with-particle spectra. Therefore, for the most accurate results, the line and continuum nonthermal radiation must be separated from the thermal signal before calculating particle temperatures.

An accompanying paper (Ref 6) identified the primary contributors to the nonthermal signals in the with-particle spectra as: 1) the radiation emitted by the plasma surrounding the particles in the detector sampling volume (designated the "perpendicular plasma signal"); 2) emission from material vaporized from the surface of the particles; and 3) where many particles are in the detector sampling volume, the particle-reflected plasma signal. With this information, a methodology has been devised whereby an approximation of the nonthermal signal is subtracted from the with-particle spectrum. This yields an improved estimate of the particle thermal emission spectrum from which a particle surface temperature can be calculated.

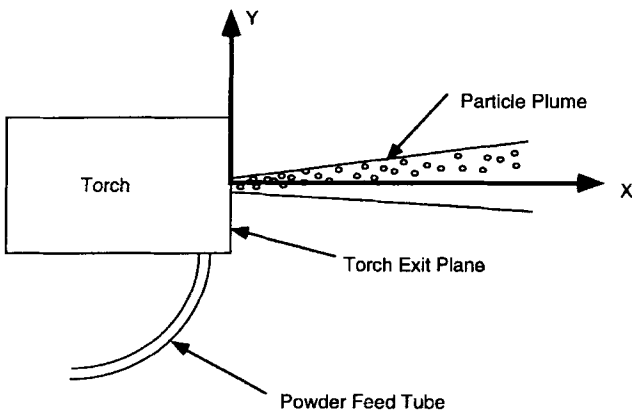

Fig. 2 Axes for spectral measurements

The general method for estimating the nonthermal component of the with-particle spectra includes the following steps. Various recorded spectra are chosen as subtraction spectra. The subtraction spectrum is used as an estimate of the nonthermal spectrum. The subtraction spectrum is subtracted from the with-particle spectrum, leaving an estimate of the particle thermal emission spectrum. This corrected thermal emission spectrum is then used to calculate the particle surface temperature. Because of the existence of nonthermal continua and line radiation, the subtraction spectrum will be a signal containing all wavelengths used for the temperature calculation. So, entire spectra will be subtracted instead of, for example, subtracting out only the line radiation that is easily identified.

The selection of possible subtraction spectra was based on information describing the signals which constitute the with-particle spectra presented in the accompanying paper (Ref 6). One component of the nonthermal signal collected by the detector is the plasma signal. This signal is a combination of the perpendicular plasma signal (plasma light normal to the spray direction) and some amount of particle-reflected plasma light in regions of high particle density. However, the perpendicular and particle-reflected plasma signals have been observed to be spectrally very similar (Ref 6). It is therefore expected that the perpendicular and particle-reflected plasma spectra, as seen in the with-particle spectra, will be very similar and can be treated as a single plasma signal for purposes of subtraction spectrum selection.

The other proposed source of nonthermal signal in the with-particle spectra is the vapor signal. This signal cannot be observed independently but only in combination with the plasma and particle thermal emission signals. A method for estimating the vapor signal has been devised. The particles undergo rapid surface heating when injected into the plasma. This rapid heating can cause evaporation of the surface material of the particles. The vapor spreads out in a cloud that surrounds the path of the particles. Beyond the region through which particles pass is the "no-particle" region. This is found directly above and below the path of the particles (Ref 6). Because there are no particles present, there is no particle thermal signal, nor is there any particle-reflected plasma light. There is, however, a signal from the particle vapor and a signal from the perpendicular plasma emission. Because an estimate of the perpendicular plasma signal is available from the without-particle spectra, the perpendicular plasma signal can be accounted for. Therefore, if the without-particle spectrum is subtracted from the with-particle spectrum (taken from the no-particle region), the result should closely approximate the vapor spectrum. The vapor spectrum determined in this way shows both peak and continuum radiation.

One choice of subtraction spectrum would contain only the plasma signal, and another choice would contain only the vapor signal. A third possible subtraction spectrum is a combination of the plasma and vapor signals. This would be especially useful in regions where neither the plasma nor vapor signals is clearly the dominant nonthermal signal present in the with-particle spectra. This combination spectrum could be constructed by combining the without-particle plasma signal with the vapor signal.

Before the various subtraction spectra can be evaluated to determine which one best represents the nonthermal signal in the with-particle spectra, one more unknown quantity must be

compensated for. The goal of subtracting the nonthermal signal from the raw data is to yield a spectrum that can be fit with a blackbody curve, from which to determine the temperature of the particles emanating from the thermal radiation. However, since the particles are not perfect blackbody radiators, compensation must be made for their spectral emittance. In many cases of thermal-sprayed particle temperature measurements, investigators have assumed that the particles exhibit gray body behavior where the spectral emittance is constant across all wavelengths (e.g., see Ref 11, 12). In this analysis, an effort was made to estimate the particle emittance and include this information in the temperature calculation.

The spectral emittance of polished pure molybdenum at various temperatures is readily available in the literature (Ref 13). However, it is likely that oxidation is occurring on the surface of the particles in view of the high affinity that molybdenum has for oxygen, especially at elevated temperatures. Even if oxidation is taking place, however, the oxide may not be clinging to the surface. If the particle surface is above the vaporization temperature of the oxide (T_{vap} = 1530 K for MoO_3) there may be no surface oxides of molybdenum. Additionally, oxidation may take place at different rates for different particles, depending on the temperature of the particles and the local availability of oxygen. The oxide layer may be forming faster or slower than the evaporation rate of the oxide. Therefore, the extent of surface oxidation is hard to determine and may vary from particle to particle.

The approach used to determine the particle emittance in this analysis was a simple one. Two spectral emittance values were used to see which gave a better blackbody fit of the corrected thermal emission data. The one with the better fit was chosen as the more accurate value. Only molybdenum and molybdenum oxide spectral emittance values were considered because the particle surface mainly consists of one of these materials. The spectral emittance value used was for solid molybdenum at 2800 K as given in the *Thermophysical Properties of Matter Handbook* (TPMH) (Ref 13). Spectral emittance values for various oxides of molybdenum are not readily available in the literature. The only spectral information found in the TPMH for molybdenum oxides is for MoO_3 at room temperature and is reported as the spectral reflectance. An estimate of the spectral emittance can be obtained by subtracting the spectral reflectance values from unity. However, whether MoO_3 is the primary oxide formed on the surface and how the reflectance values change as the temperature increases are not known.

4.2 Method for Evaluation of the Subtraction Spectra and the Emittance Values

After the particle surface spectral emittance had been chosen, the postulated subtraction spectra were evaluated to see which combination most closely approximated the actual nonthermal signal. The subtraction spectrum to be evaluated is subtracted from the with-particle spectrum. The resulting spectrum is then curve fit using a blackbody radiation curve which has been corrected for the emittance of the particles. The quality of the blackbody fit is an indication of how well the chosen subtraction spectrum matches the shape and intensity of the nonthermal signal. The subtraction spectrum is then multiplied by a constant and again subtracted from the with-particle spectrum. The multiplying constant is determined by observing the quality of the blackbody fit and postulating whether more or less intensity must be subtracted for a better fit of the data. This new difference spectrum is again curve fit using a blackbody radiation spectrum. This process is repeated until the multiple of the proposed subtraction spectrum that gives the best blackbody fit is found. This entire process of subtraction spectrum multiplication and blackbody curve fitting is repeated for all of the proposed subtraction spectra. The quality of fit for each of the proposed subtraction spectra are compared, to determine which of the spectra most closely resembles the nonthermal signal present. The subtraction spectrum that gives the best blackbody fit is then subtracted from the with-particle spectrum, yielding a difference spectrum that represents the thermal signal upon which the particle temperature calculation is based.

In order to determine which spectral emittance value (that for molybdenum or that for MoO_3) most closely resembles the actual particle spectral emittance, the quality of fit of the with-particle spectra to the blackbody curve was considered. Because more accurate spectral emittance data are available for the pure molybdenum than for the oxides, the metal spectral emittance was used as the first estimation. Once the best subtraction spectrum has been determined, the emittance is evaluated. If the use of the oxide emittance substantially changes the quality of the blackbody fit, then the better value for spectral emittance can be determined. As seen in Fig. 3, the two values for spectral emittance are quite similar except for wavelengths less than 450 nm. This low wavelength region should be a good testing region to see if the data better fits the molybdenum or the MoO_3 emittance values.

4.3 Blackbody Curve Fitting for Subtraction Spectrum Determination

The first step in blackbody curve fitting is to choose the spectrum to be subtracted from the with-particle data. Next, each spectrum is corrected for emittance using the molybdenum spectral emittance value at 2800 K. Finally, the curve fit is performed by finding the least squares blackbody fit to the given spectrum.

The curve-fitting routine finds the temperature of the blackbody spectrum which best fits the shape of the given collected spectrum. The computer software package KaleidaGraph (Synergy Software, Reading, PA), which utilizes the Levenberg-Marquardt algorithm

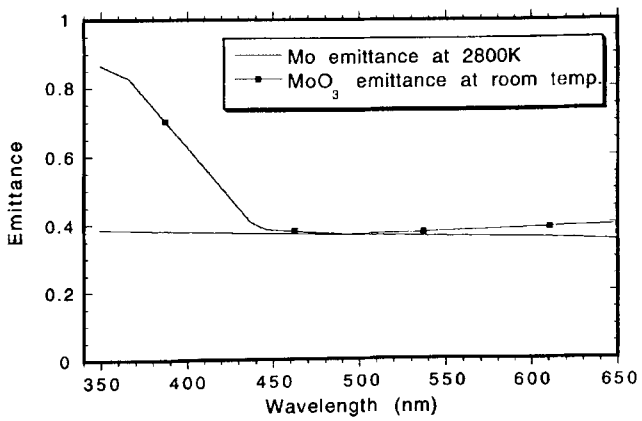

Fig. 3 Spectral emittance values for Mo and MoO_3 (Ref 13)

for general nonlinear curve fitting, is used. The absolute intensity of the spectra has no effect on the fitting process because the shape of the spectra alone is used to calculate the temperature. The best fit temperature along with the quality of the fit indicated by the Pearson's r value are given for each spectrum fit. Pearson's r value is calculated:

$$r = \frac{\sum_{i}^{N} (x_i - \bar{x})(y_i - \bar{y})}{\sqrt{\sum_{i}^{N} (x_i - \bar{x})^2} \sqrt{\sum_{i}^{N} (y_i - \bar{y})^2}} \quad \text{(Eq 2)}$$

where x_i is the calculated intensity value, y_i is the actual intensity value, $\bar{x}$ is the mean of the calculated intensity values, $\bar{y}$ is the mean of the actual intensity values, and the index i goes from one to the total number of data points used in the curve fit, N. A Pearson's $r = 1$ means that the fit and the raw data perfectly coincide. The Pearson's r value using one subtraction spectrum is compared to the Pearson's r value using another subtraction spectrum for the same with-particle spectrum. The subtraction spectrum which gives the better fit (larger r value) is assumed to be more representative of the nonthermal signal. By continuing this process for all postulated subtraction spectra, the subtraction spectrum which most closely represents the nonthermal signal is determined. The spatial location chosen for the initial subtraction spectrum determination is at $x = 80$ mm, $y = 5.5$ mm. This location is near the maximum intensity, which indicates that it is near the maximum particle flux y-location for this x-location. Each of the proposed subtraction spectra were tested using the with-particle spectrum taken at this location.

As a reference case, the with-particle spectrum was fit to the blackbody spectrum without any subtraction spectrum. The with-particle and best fit blackbody spectra are shown in Fig. 4. The quality of fit is given by a Pearson's $r = 0.9988$. The temperature of the best fit blackbody was found to be 3185 K. The melting point of molybdenum metal is 2880 K.

The first subtraction spectrum tested was the without-particle plasma signal. This spectrum is shown in Fig. 5. The quality of fit is given by a Pearson's $r = 0.99940$. The temperature of the best fit blackbody was found to be 2990 K. This quality of fit represents an improvement over the reference case of the raw with-particle spectrum. This means that the effort to decrease the nonthermal signal by using a subtraction spectrum in the data is likely working.

The subtraction and fitting process was repeated, this time using the vapor signal for the subtraction spectrum. The vapor signal was determined by subtracting the without-particle spectrum from the with-particle spectrum at a location just outside the edge of the trajectory of the particles (no-particle region) closest to the torch centerline ($x = 80$ mm, $y = 0$ mm). The vapor signal is shown in Fig. 6. The quality of fit is given by a Pearson's $r = 0.99917$. The temperature of the best fit blackbody was found to be 3125 K. Figure 6 also shows the final subtraction spectrum and the final curve-fit temperature spectrum. Using the vapor signal as the subtraction spectrum gave a better fit than the raw data but was not as good as using the without-particle plasma signal as the subtraction spectrum.

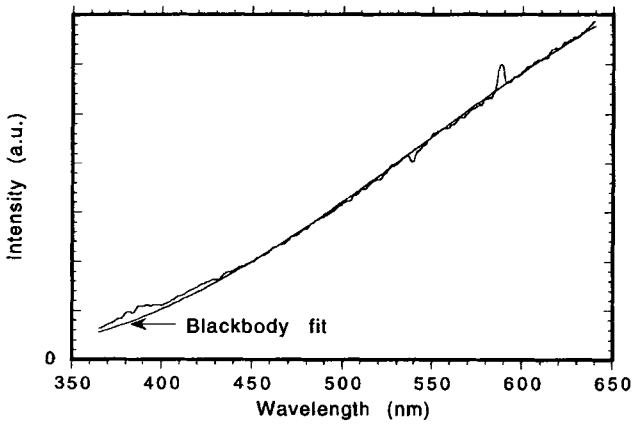

Fig. 4 With-particle and blackbody curve fit (smooth curve) spectra at $x = 80$ mm, $y = 5.5$ mm. The curve fit yields a temperature of 3185 K with a Pearson's $r = 0.9988$.

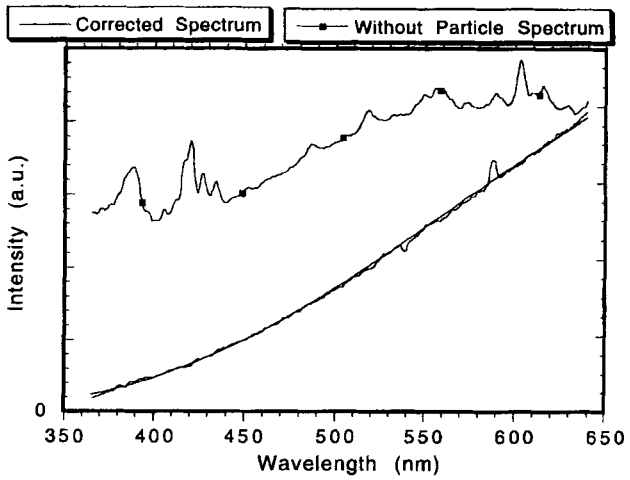

Fig. 5 Without-particle and corrected thermal emission spectrum (plotted on different scales) with blackbody fit (smooth curve) for location $x = 80$ mm, $y = 5.5$ mm. The curve fit yields a temperature of 2990 K with a Pearson's $r = 0.99940$.

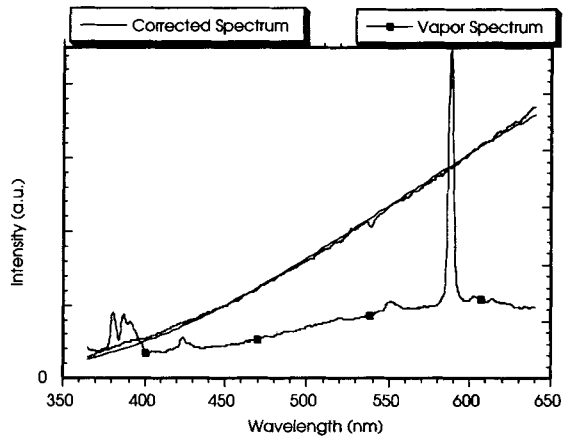

Fig. 6 Vapor and corrected thermal emission spectrum (plotted on different scales) with blackbody fit (smooth curve) for location $x = 80$ mm, $y = 5.5$ mm. The curve fit yields a temperature of 3125 K with a Pearson's $r = 0.99917$.

A third spectrum, which consists of a combination of the plasma and vapor signals, was proposed for use as the subtraction spectrum. This combination of signals is found in the with-particle spectrum in the no-particle region. Because it was shown in the accompanying paper "Analysis of the Non-Thermal Emission Signal Present in a Molybdenum Particle Laden Plasma-Spray Plume" that the vapor signal can vary with position away from the torch centerline (Ref 6), it is likely that the plasma-plus-vapor signal on the side of the particle trajectory opposite the torch centerline has a different shape than the corresponding signal near the torch centerline. The plasma-plus-vapor signals for positions in the no-particle regions on the torch centerline side ($y = 0$ mm) and the opposite side ($y = 15.3$ mm) are shown in Fig. 7. From the figure it is evident that the spectra vary significantly with position. Since the particles lie between the positions where these two spectra were recorded, it is likely that the nonthermal signal in the vicinity of the particles varies from the spectrum near the torch centerline to the spectrum on the opposite side. A linear combination of these two plasma-plus-vapor spectra may be a better representation of the nonthermal signal than any single subtraction spectrum used across the entire y-range. In the temperature-fitting process, the linear combination subtraction spectrum that best fit the data was used.

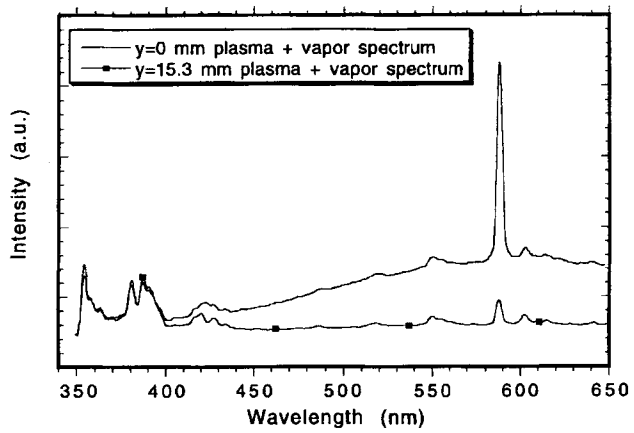

Fig. 7 Plasma-plus-vapor spectra above and below the particle trajectories

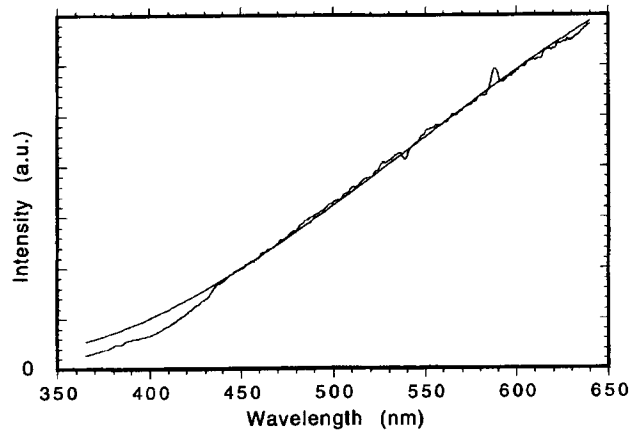

Fig. 9 Best blackbody fit (smooth curve) and corrected spectrum using the spectral emittance of MoO_3. The curve fit yielded a temperature of 3168 K with a Pearson's $r = 0.99714$.

This process requires more iteration, but yields the best fit subtraction spectrum, the temperature, and the Pearson's r for each location in the plume. The best fit subtraction spectrum for the spectrum taken at $x = 80$ mm, $y = 5.5$ mm was found to be the linear combination of one part of the $y = 15.3$ mm subtraction spectrum and three parts of the $y = 0$ mm subtraction spectrum. The corresponding temperature was calculated to be 3074 K with a Pearson's $r = 0.99953$. The final corrected spectrum and the best blackbody curve fit are shown in Fig. 8. This linear combination subtraction spectrum which accounts for both plasma and vapor nonthermal signals achieved the best blackbody fit of the spectra tested. Figure 8 also shows a slight line absorption of the thermal radiation near 538 nm. This is assumed to be due to absorption from an unidentified plasma or vapor species.

4.4 Particle Emittance Evaluation

Using the linear combination subtraction spectrum to account for the nonthermal signal present, the question of particle emittance can again be addressed. The MoO_3 emittance, instead of the molybdenum emittance, was used to determine which gives the better blackbody curve fit. The same with-particle

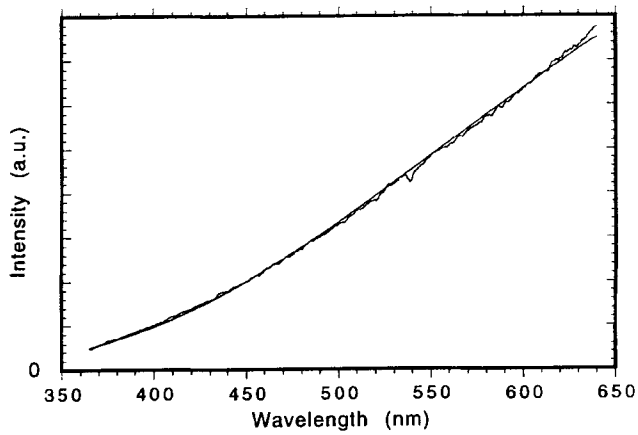

Fig. 8 Best blackbody fit (smooth curve) and corrected spectrum using the linear combination plasma plus vapor subtraction spectrum. The curve fit yielded a temperature of 3074 K with a Pearson's $r = 0.99953$.

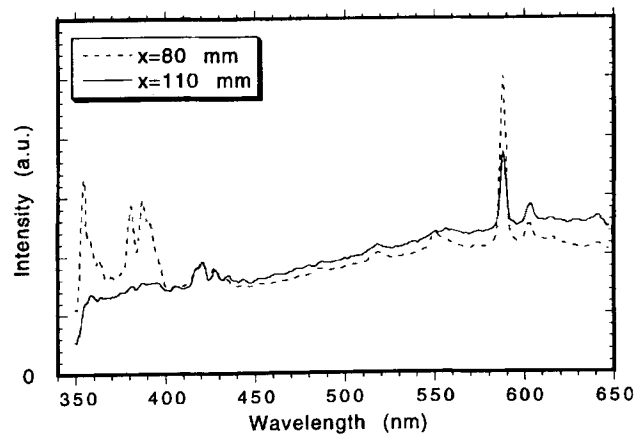

Fig. 10 Representative subtraction spectra for $x = 80$ and 110 mm

spectrum that was used for determining the best subtraction spectrum ($x = 80$ mm, $y = 5.5$ mm) was used to determine the better emittance value. Using the MoO_3 emittance value and the linear combination of plasma-plus-vapor signal as the subtraction spectrum, the temperature of the best fit was 3168 K, with a Pearson's $r = 0.99714$. The spectrum corrected for emittance using the MoO_3 value along with the best blackbody fit are shown in Fig. 9. A comparison of this fit to Fig. 8, which uses the same subtraction spectrum but the emittance of molybdenum, shows a much better fit using the emittance value for molybdenum. The blackbody fit to the MoO_3 corrected spectra is especially poor in the spectral region below 450 nm where the two emittance values diverge. This divergence from the blackbody shape indicates that the sharp rise in the MoO_3 emittance below 450 nm is not consistent with the thermal signal recorded. Therefore, the spectral emittance value for molybdenum is the better one to use for the reduction of the data collected in this experiment. There may be some amount of oxide on the surface of the particles, but it appears from the emittance comparison that either it is not MoO_3 or that there is significantly more metallic molybdenum than oxide on the surface. The gray-body relation for spectral emittance was also evaluated. It gave about the same quality of fit as the molybdenum emittance. Therefore, the literature value of emittance for molybdenum and the gray-body assumption are about equally accurate for the data investigated. However, for the analysis presented here, the molybdenum emittance was used.

4.5 Applying the Subtraction Spectrum and Emittance to the Data

The linear combination of the plasma-plus-vapor subtraction spectrum, along with the molybdenum emittance value, gives the best blackbody fit to the with-particle data as evidenced by a comparison of the Pearson's r values. Representative subtraction spectra determined for $x = 80$ and 110 mm are shown in Fig. 10. The subtraction spectra for $x = 140$, 170, and 200 mm are nearly identical to each other. They are also very similar to the subtraction spectrum for $x = 110$ mm except that they have far less intensity for line emission at 589 nm. The subtraction spectra at these locations ($x = 140$ to 200 mm) closely resemble the perpendicular plasma signal indicating that the plasma signal is the dominant nonthermal signal present. The subtraction spectrum for $x = 110$ mm is also similar to the perpendicular plasma signal except for the strong sodium line at 589 nm. Therefore, both the plasma and the vapor signals contribute significantly to the nonthermal signal at $x = 110$ mm. The subtraction spectrum at $x = 80$ mm shows an even stronger sodium line. In addition, chromium and molybdenum lines in the 350 to 400 nm region are clearly visible. Therefore, for the purposes of achieving the best temperature fit, the $x = 80$ mm subtraction spectrum can probably best be described as vapor-signal dominant. In determining the subtraction spectrum as a function of distance downstream from the torch exit, it becomes clear that the vapor signal dominates near the torch exit and the plasma signal dominates far from the torch exit. In between these extremes, both components contribute significantly to the nonthermal signal.

Using the method described above for determining the best linear combination subtraction spectrum of plasma-plus-vapor signal, the other spectra at the $x = 80$ mm location were fit to a blackbody curve. The resulting temperatures are shown in Fig. 11. Pearson's r values are shown in Table 2. The consistency of the Pearson's r values represent a reproducible quality of fit, supporting the notion that the subtraction spectrum is being changed in a way consistent with the change of the nonthermal signal in the data. The temperatures at the other x-locations were

Table 2 Pearson's r values for the corrected fit thermal spectra as a function of x and y position and for the uncorrected spectra at $x = 80$ mm

y-Position, mm	$x = 80$ mm corrected	$x = 80$ mm uncorrected	$x = 110$ mm corrected	$x = 140$ mm corrected	$x = 170$ mm corrected	$x = 200$ mm corrected
$y = 3.3$	0.99939	0.93968	0.99953	...	...	...
$y = 4.4$	0.99951	0.99821	0.99957	0.99970	0.99957	0.99915
$y = 5.5$	0.99953	0.99873	0.99955	0.99967	...	...
$y = 6.5$	0.99962	0.99919	0.99966	0.99975	0.99972	0.99976
$y = 7.6$	0.99944	0.99901	0.99959	0.99971	0.99967	...
$y = 8.7$	0.99959	0.99887	0.99960	0.99976	...	0.99977
$y = 9.8$	0.99947	0.99512	0.99958	0.99968	0.99971	0.99976
$y = 10.9$	0.99947	0.96241	0.99960	0.99981	0.99976	0.99977
$y = 11.9$	...	...	0.99952	0.99968	0.99973	0.99978
$y = 13.0$	...	...	0.99965	0.99971	0.99974	0.99978
$y = 14.1$	...	...	0.99958	0.99976	0.99973	0.99974
$y = 15.2$	...	...	0.99958	0.99976	0.99979	0.99974
$y = 16.35$	...	...	...	0.99979	0.99977	0.99975
$y = 17.4$	...	...	...	0.99974	0.99977	0.99968
$y = 18.5$	...	...	...	0.99984	0.99980	0.99976
$y = 19.6$	...	...	...	...	0.99977	0.99978
$y = 20.7$	...	...	...	...	0.99979	0.99982
$y = 21.8$	...	...	...	...	0.99980	0.99985
$y = 22.8$	...	...	...	...	0.99977	0.99980
$y = 23.9$	...	...	...	...	0.99976	0.99985
$y = 25.1$	...	...	...	...	0.99943	0.99981
$y = 26.2$	...	...	...	...	...	0.99982
$y = 27.3$	...	...	...	...	...	0.99982
$y = 28.3$	...	...	...	...	...	0.99955

determined in a similar way. The temperatures at x =110, 140, 170, and 200 mm, are shown in Fig. 12 to 15. Because the spectra were not smoothed before fitting, the good quality of fit seen in Table 2 represents good physical coincidence between the corrected with-particle spectra and the blackbody radiation curves.

Using the various subtraction spectra and the uncorrected data for the location x = 80 mm, y = 5.5 mm gives temperatures which are within 6% of each other. This may seem small given the assumptions made in the analysis, but when the uncorrected temperature values are compared to the corrected values for all y-locations, the corrected data begin to differ to a larger degree. Figure 11 shows the corrected and uncorrected data for the location x = 80 mm. Near the center of the particle distribution, where the particle signal is strongest (y = 7.6 mm), the error between the two temperatures is smallest (1.5% or 45 K). At the edges of the distribution where there are fewer particles (y = 10.9 mm), the error is largest (14% or 420 K). A similar trend in temperature difference is observed for the other x-locations. In all cases, the Pearson's r values for the corrected spectra are much higher than the values for the uncorrected spectra, as seen in Table 2 for the data at x = 80 mm. Therefore, the nonthermal correction process is most useful where there are fewer particles (or comparatively more nonthermal signal) in the detector field of view. It is also expected that at locations closer to the exit of the torch where the nonthermal emission signal is stronger, the correction process will significantly improve the accuracy of particle temperature data. This hypothesis will be tested in future work.

The error in the temperature data comes from several sources. The data point at x = 170 mm, y = 14.2 mm will be used as an example of error calculation. The first error source comes from the IRF calculation. The calibrated lamp used had an accuracy of 1% at 2500 K which is the temperature used for determining the IRF. The 25 K uncertainty in the lamp temperature carries over into the particle temperature uncertainty. The next source of error is the particle emittance. As shown in the preceding discussion, the temperature determined for the data point at x = 80 mm, y = 5.5 mm using the emittance for molybdenum is 3074 K, whereas the temperature determined using the emittance of MoO_3 is 3168 K. A similar temperature difference is expected for the data point at x = 170 mm, y = 14.2 mm. However, as was shown above, the emittance of molybdenum is much closer to the actual emittance of the particle than is the emittance for MoO_3. The estimated temperature error due to emittance is ~25 K. The final source of error for the temperature measurements is the choice of subtraction spectra. At x = 170 mm, y = 14.2 mm, using the linear combination subtraction spectrum, the temperature is 3010 K. If the without-particle signal is used for the subtraction spectrum, the resultant particle temperature is 3020 K. If no subtraction spectrum is used the calculated particle temperature is 3075 K. Since the careful choice of subtraction spectrum can reduce this source of error, it is estimated that the uncertainty added to the data point at x = 170 mm, y = 14.2 mm

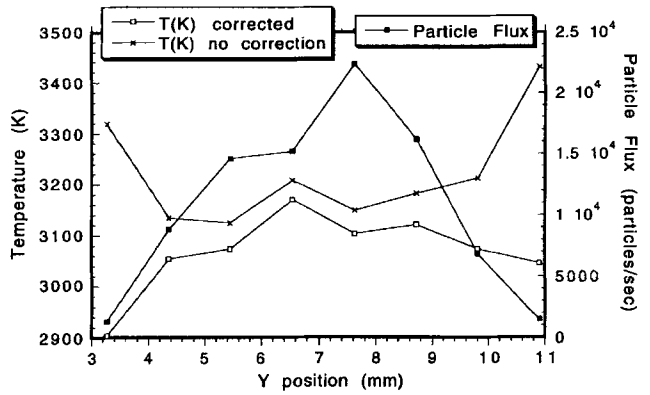

Fig. 11 Corrected and uncorrected temperature and particle flux at x = 80 mm

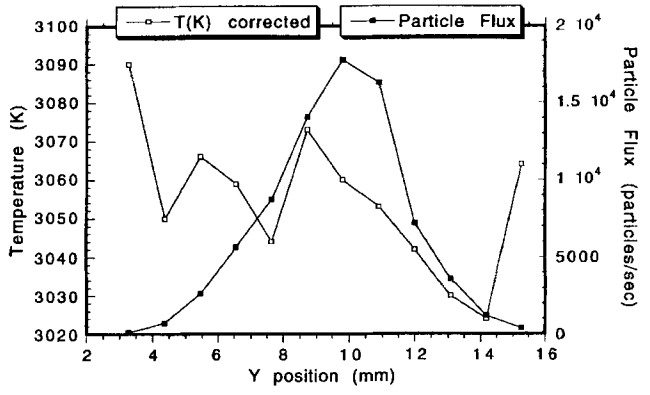

Fig. 12 Particle temperature and particle flux for x = 110 mm

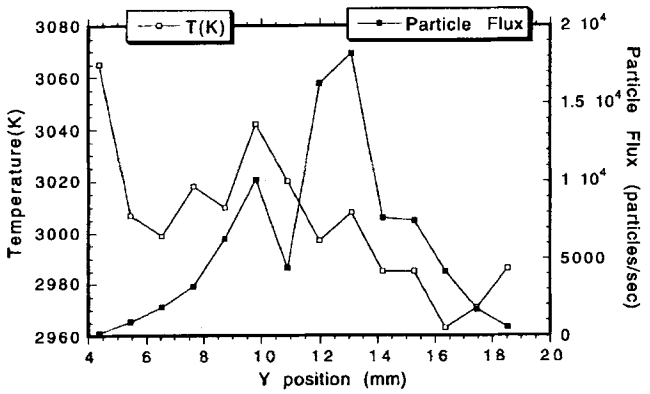

Fig. 13 Particle temperature and particle flux for x = 140 mm

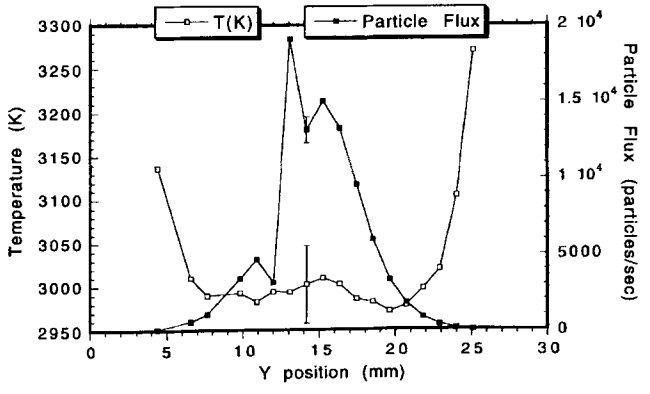

Fig. 14 Particle temperature and particle flux for x = 170 mm

is about 30 K. Combining the squares of these three errors and then taking the square root of the sum gives a combined temperature error of 46 K which corresponds to a 1.5% uncertainty. Figure 14 shows a representative temperature error bar on the point used as an example here.

4.6 Treatment of High-Temperature Edge Particles

The high temperatures recorded on the edge of the particle plume for $x \geq 110$ mm were not expected (Fig. 12-15). Because there are very few particles in the edge region, the high temperatures may erroneously result from some unknown nonthermal signal which is insignificant at locations with more particles. However, the consistent Pearson's r values out to the edge, as seen in Table 2, indicate that the blackbody match remains good. Also, at $x = 80$ mm, the edge particle temperatures do not rise. The data also indicate a trend of increasing edge particle temperatures as distance from the torch exit increases.

To determine the extent to which the selection of the subtraction spectrum affects the rise of calculated particle temperatures on the edge of the plume, all subtraction spectra were utilized for fitting the temperature of the particles at $x = 170$ mm, where a large temperature rise was noted. The various subtraction spectra and emittance values used changed the absolute value of temperature determined for each point but did not significantly change the rising temperature of particles at the edge of the plume. Therefore, it is concluded that the choice of subtraction spectrum and emittance value is not causing the high calculated temperatures on the edge of the particle plume.

It seems likely that there may be some particles on the very edge of the plume that are getting much hotter than the other particles. These hot particles may be due to increased in-flight oxidation occurring on the surface of these particles. Because the edge of the plume has fewer particles, there is less competition for the oxygen that is present. As the particles move downstream, they encounter higher oxygen partial pressures and have had more time at elevated temperatures to undergo oxidation, which leads to higher surface temperatures. The increase in local oxygen partial pressure is due to two factors. First, as the particles travel downstream, they fan out away from the torch centerline into areas where there is more air and less of the inert torch gas. The other factor is the entrainment of air into the plasma jet after the onset of turbulence some distance downstream from the torch exit. Thus, the closer to the torch (smaller x), the less oxidation is expected to take place. This trend is confirmed in the temperature measurements in Fig. 12 to 15 which show an increase in edge particle temperatures as the distance from the torch exit increases.

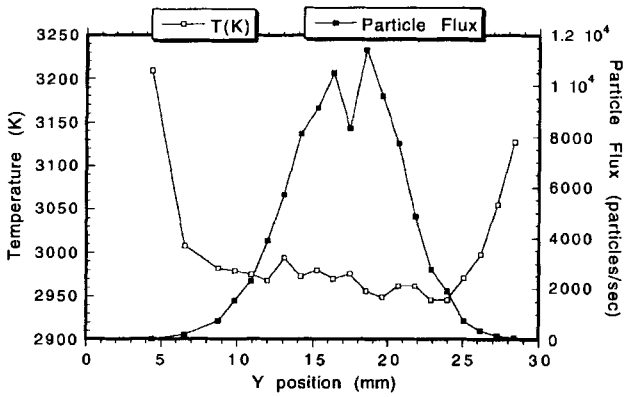

Fig. 15 Particle temperature and particle flux for $x = 200$ mm

4.7 Particle Flux Calculation

As demonstrated above, the multi-color temperature measurement technique determines the particle temperature by the shape of the thermal spectrum emitted by the particles. Although the absolute intensity of the collected spectra has not been used, it contains important information which need not be discarded. Assuming a constant emittance for all particles at a given x-location, the absolute intensity of the thermal spectra for particles of a narrow size distribution is a function of the particle temperature and the number of particles observed. Therefore, the measured intensities and the calculated temperatures can be used to give an estimate of the number of particles passing through the sampling volume. The equation relating these values is again the Planck equation, rearranged to give particle number, but only a single wavelength of radiation is needed for the calculation:

$$n = \frac{I\lambda^5[\exp(C_2/\lambda T) - 1]}{2\pi C_1} \qquad \text{(Eq 3)}$$

where n is the relative number of particles observed, I is the detected intensity at a given wavelength, λ is the wavelength, T is the absolute temperature, and c_1 and c_2 are the first and second constants in Planck's spectral energy distribution.

The previously determined particle temperatures along with the intensity at a given wavelength (472 nm, chosen arbitrarily for this analysis) are sufficient to determine the relative particle flux for each location in the plume. This relative particle flux figure can be turned into the actual particle flux since the actual mass feed rate, particle size, and material density are known. Assuming that all of the particles are detected, the actual number of particles passing through the sampling volume per unit of time was calculated. Figures 11 to 15 show the results of the particle flux calculations for $x = 80$, 110, 140, 170, and 200 mm. As shown in the figures, the particles are most numerous in the central portion of the plume and decrease in number toward the edges. Also, the peak particle number decreases, and the spreading of the particle plume in the y-direction increases, as the distance from the torch exit increases. These optical measurements are consistent with the spray patterns observed in spraying at various x-distances with the torch held stationary relative to the substrate. The sprayed samples showed a broadening of the deposit as the distance from the torch exit plane increased, just as the optical measurements show. Also evident in the figures are locations of unexpectedly low particle flux, such as at $x = 140$ mm, $y = 11$ mm (Fig. 13). These are due to fluctuations in the particle feed rate and represent the particle flux when the spectrum was taken. However, if averaged over a longer signal integration time, the particle flux distribution would vary smoothly with the y-coordinate.

The primary error in the particle flux measurements comes from the uncertainty in particle temperature. For the data point at $x = 170$ mm, $y = 14.2$ mm which has a particle flux of ~1.5×10^4 particles/s, the uncertainty in temperature was previously shown to be 46 K. The error in particle flux which results from

this temperature uncertainty is 1800 particles/s. This corresponds to an error of 12%. Figure 14 shows a representative particle flux error bar on the point used as an example here. The particle flux values represent only the hot particles because the cool particles are not detected by this technique.

4.8 *The Averaged Nature of Temperature Measurements*

At this point the exact nature of the particle temperature and flux measurements should be explained in more detail. As Fig. 2 shows, the optical emission is sampled through chords in the plasma/particle plume. Therefore, the observed thermal signal is not for particles at a single location, but for all particles in the line of sight of the detector.

Because it is unlikely that all particles in the sampling volume have the same temperature, the calculated particle temperature is not the temperature of the particles at any one location along the detector line of sight. Instead, the calculated temperature is a weighted average of the temperature of all particles detected. The calculated temperature is not a linear average of the actual particle temperatures; instead, it is more heavily influenced by the higher-temperature particles present. This weighting is demonstrated most easily by example. Figure 16 shows the blackbody emission spectra for 2800, 3000, and 3200 K. Because this is the general range of particle temperatures calculated previously, the majority of actual particle temperatures likely fall within this range. A thermal spectrum was constructed by adding together the thermal signals of single "particles." The "particles" ranged in temperature from 2800 to 3200 K in 25° intervals for a total of 17 particles. This combination spectrum is similar to what is actually detected from the particle plume. The combination spectrum was fit using the blackbody function to give a temperature of 3040 K, which is higher than the average temperature of the "particles" of 3000 K. The deviation from the true average in this case is 1.3%. Higher-temperature particles emit more radiation than lower-temperature particles, as demonstrated in the Stefan-Boltzmann law. The larger amount of radiation gives the hotter particles more weight when averaging, thus the fit temperature is higher than the unweighted average temperature. Because this calculation is close to the actual experimental conditions, it is expected that the measured temperatures differ from the average temperature of the particles by less than 2%. The blackbody fit to the combination spectrum has a Pearson's r value of 0.999999 indicating a very good fit. This good fit indicates that even though particles of various temperatures make up the combination spectrum, the resultant signal closely resembles that of a single blackbody radiator at the fit temperature. This means that the particle thermal measurements should fit an emittance-corrected blackbody curve quite well, even though the signal is made up of thermal signals of various temperatures.

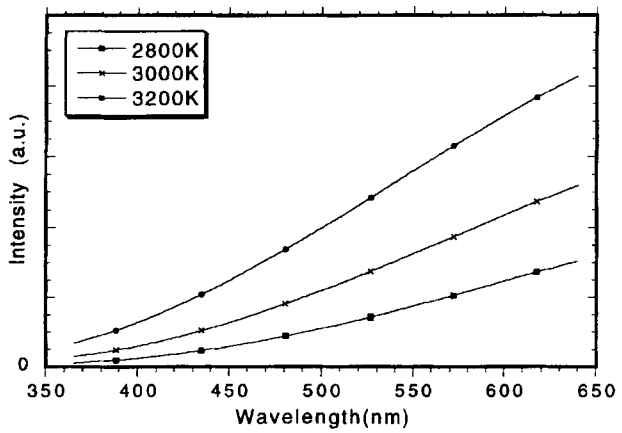

Fig. 16 Blackbody spectra for particles at 2800, 3000, and 3200 K

Because the particle flux calculation is based on the calculated temperature values, it, too, is not an exact representation of particle flux. Instead, it varies slightly from the actual particle number because all of the particles are not at one single temperature, as the calculation method assumes. Following the example in Fig. 16, the difference in actual and calculated particle flux can be seen. The actual number of particles in the example is 17 (one particle at each temperature). The calculated number assumes that all particles are at the same temperature determined from the curve fit (3040 K). The calculated number of particles, using Eq 2, is 15.9. Therefore, the error in the particle number calculation is 6.5%. Although the error is not particularly large, it is representative of the fact that it is not the actual number of particles that is calculated, but some quantity that is closely related to the actual number.

5. Conclusions

The research presented here yielded the following results.

- The presence of vapor and plasma signals in spectra collected for particle pyrometry can cause significant errors in temperature calculations using two-color or multi-color pyrometry. Therefore, to minimize temperature errors, both plasma and vapor lines should be considered when selecting wavelength bands for pyrometry.
- The nonthermal signal present was found to be best approximated by a combination of the plasma and vapor signals present. The vapor signal is strongest near the torch (80 mm downstream from the torch exit), while the plasma signal dominates further downstream (140 to 200 mm from the torch exit).
- The spectral emittance of the molybdenum particles in flight was found to resemble the spectral emittance of molybdenum more than the spectral emittance of MoO_3. The gray-body assumption for the spectral emittance of the particles was shown to give about the same results as the spectral emittance for molybdenum.
- The line-averaged temperature of particles in the region from 80 to 200 mm downstream of the torch exit was calculated from the corrected raw spectra.
- The line-averaged particle flux was calculated for the region from 80 to 200 mm downstream of the torch exit. The measured distribution agrees with the spray pattern produced on a substrate held stationary with respect to the torch.
- A new technique was developed for the measurement of particle temperatures. By subtracting the nonthermal signal from the collected spectra, more accurate particle temperatures could be calculated. The ability to estimate and remove nonthermal signals may allow for temperature measurements to be made closer to the exit plane of the torch than are now possible, thus allowing exploration of previously undocumented areas.

Acknowledgments

This research was performed under appointment to the Magnetic Fusion Energy Technology Fellowship program administered by Oak Ridge Institute for Science and Education for the U.S. Department of Energy. This work was performed at Sandia National Laboratories, operated by Lockheed Martin for the U.S. Department of Energy under contract DE-AC04-94AL85000.

References

1. M. Vardelle, A. Vardelle, A.C. Leger, and P. Fauchais, Dynamics of Splat Formation and Solidification in Thermal Spraying Process, *Thermal Spray Industrial Applications,* C.C. Berndt and S. Sampath, Ed., ASM International, 1994, p 555-562
2. R. McPherson, A Review of Microstructure and Properties of Plasma Sprayed Ceramic Coatings, *Surf. Coat. Technol.,* Vol 39 (No. 40), 1989, p 173-181
3. J. Mishin, M. Vardelle, J. Lesinski, and P. Fauchais, Two-Colour Pyrometer for the Statistical Measurement of the Surface Temperature of Particles Under Thermal Plasma Conditions, *J. Phys. E, Sci. Instrum.*, Vol 20, 1987, p 620-625
4. S. Kuroda, T. Fukushima, S. Kitahara, H. Fujimori, Y. Tomita, and T. Horiuchi, Monitoring of Thermally Sprayed Particles Using Thermal Radiation, Vol 2, Paper 27, *Proc. 12th Int. Conf. on Thermal Spraying,* I.A. Bucklow, Ed., The Welding Institute, Cambridge, UK, 1989
5. J.R. Fincke, W.D. Swank, and C.L. Jeffery, Simultaneous Measurement of Particle Size, Velocity, and Temperature in Thermal Plasmas, *IEEE Trans. on Plasma Sci.,* Vol 18 (No. 6), 1990 p 948-957
6. K.J. Hollis and R.A. Neiser, Analysis of the Nonthermal Emission Signal Present in a Molybdenum Particle Laden Plasma-Spray Plume, *J. Therm. Spray Technol.,* Vol 7 (No. 3), p 383-391
7. K.J. Hollis and R.A. Neiser, Spectral Analysis of a Molybdenum Particle Laden Plasma Plume, *Advances in Thermal Spray Science & Technology,* C.C. Berndt and S. Sampath, Ed., ASM International, 1995, p 129-134
8. T. Sakuta and M.I. Boulos, Novel Approach for Particle Velocity and Size Measurement Under Plasma Conditions, *Rev. Sci. Instrum.,* Vol 59 (No. 2), 1988, p 285-291
9. P. Gougeon and C. Moreau, In-Flight Particle Surface Temperature Measurements: Influence of the Plasma Light Scattered by the Particles, *Thermal Spray Coatings: Research, Design and Applications,* C.C. Berndt and T.F. Bernecki, Ed., ASM International, 1993, p 13-18
10. J. Prucha and Z. Skarda, The Improvement of the Spectroscopical Temperature Diagnostic of Plasma Sprayed Particles, *Thermal Spray: International Advances in Coatings Technology,* C.C. Berndt, Ed., ASM International, 1992, p 343-348
11. H. Hantzsche, "Temperature Measurement of Powder Particles in a Plasma Jet," Paper 16, Vol 1, *Proc. of Seventh Int. Metal Spraying Conf.,* The Welding Institute, Cambridge, UK, 1973
12. X. Xu, G. Chen, and Y. Shen, Surface Temperature Diagnostics for Plasma Spray in an Inert Environment, *Proc. of First Plasma Technik Symposium,* H. Eschnauer, P. Huber, A. Nicoll, and S. Sandmeier, Ed., Plasma-Technik AG, Wohlen, Switzerland, 1988, p 99-103
13. Y.S. Touloukian and D.P. DeWitt, *Thermophysical Properties of Matter,* IFI/Plenum, 1970